Mineral changes in cement-sandstone matrices induced by biocementation

C. Verba [a,*], A.R. Thurber [b], Y. Alleau [b], D. Koley [c], F. Colwell [b], M.E. Torres [b]

[a] National Energy Technology Laboratory, U.S. Department of Energy, OR 97321, USA
[b] College of Earth, Ocean, and Atmospheric Sciences, Oregon State University, OR 97330, USA
[c] College of Science, Oregon State University, OR 97330, USA

ABSTRACT

Prevention of wellbore CO_2 leakage is a critical component of any successful carbon capture, utilization, and storage program. *Sporosarcina pasteurii* is a bacterium that has demonstrated the potential ability to seal a compromised wellbore through the enzymatic precipitation of $CaCO_3$. Here we investigate the growth of *S. pasteurii* in a synthetic brine that mimics the Illinois Basin and on Mt. Simon sandstone encased in Class H Portland cement under high pressure and supercritical CO_2 (P_{CO2}) conditions. The bacterium grew optimum at 30 °C compared to 40 °C under ambient and high pressure (10 MPa) conditions; and growth was comparable in experiments at high P_{CO2}. *Sporosarcina pasteurii* actively induced the biomineralization of $CaCO_3$ polymorphs and $MgCa(CO_3)_2$ in both ambient and high pressure conditions as observed in electron microscopy. In contrast, abiotic (non-biological) samples exposed to CO_2 resulted in the formation of surficial vaterite and calcite. The ability of *S. pasteurii* to grow under subsurface conditions may be a promising mechanism to enhance wellbore integrity.
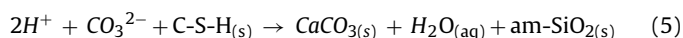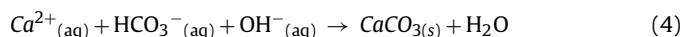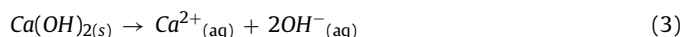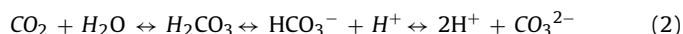
Published by Elsevier Ltd.

1. Introduction

Carbon sequestration pilot programs are being conducted to evaluate the injection of carbon dioxide (CO_2) into deep geological formations to mitigate the rise in atmospheric CO_2 concentrations. During carbon sequestration, it is essential to maintain wellbore integrity to prevent the injected CO_2 from leaking either into adjacent formations or being released back into the atmosphere (e.g. McGrail et al., 2006). Several pathways exist in which CO_2 leakage could lead to groundwater or surficial aquifer contamination, but the probability of CO_2 leakage is greater at the cement-host lithologies interface, around the annulus, and at the cement plug (e.g. Duguid et al., 2011; Gasda et al., 2013).

Class G or H Portland cement paste is used in oil and gas wells and is composed of unhydrated calcium silicates, calcium aluminoferrites, magnesium oxide phases, and hydrated phases such as calcium hydroxide ($Ca(OH)_2$) or semi-amorphous calcium silicate hydrate (known as C–S–H in cement nomenclature) (Taylor, 1997). Carbon dioxide injected during carbon capture and storage (CCUS) exists as a supercritical fluid at depths greater than 800 m where critical pressures (>7.38 MPa), and temperatures (>31.1 °C) exist.

Several studies have documented alteration of hydration products in the cement paste in the presence of supercritical CO_2 and CO_2-saturated brine (e.g. Kutchko et al., 2008; Barlet-Gouedard et al., 2009). Furthermore, poor bonding or emplacement of cement combined with supercritical CO_2 conditions may reduce the effectiveness of carbon capture. The reaction of CO_2 with cement is provided below with Eqs. (1)–(5) (Kutchko et al., 2008). This is a two-step process where the formation of carbonic acid results in the dissolution of $Ca(OH)_2$, and subsequently the conversion of C–S–H into amorphous silica gel.

$$CO_{2(g)} \rightarrow CO_{2(aq)} \tag{1}$$

$$CO_2 + H_2O \leftrightarrow H_2CO_3 \leftrightarrow HCO_3^- + H^+ \leftrightarrow 2H^+ + CO_3^{2-} \tag{2}$$

$$Ca(OH)_{2(s)} \rightarrow Ca^{2+}_{(aq)} + 2OH^-_{(aq)} \tag{3}$$

$$Ca^{2+}_{(aq)} + HCO_3^-_{(aq)} + OH^-_{(aq)} \rightarrow CaCO_{3(s)} + H_2O \tag{4}$$

$$2H^+ + CO_3^{2-} + \text{C-S-H}_{(s)} \rightarrow CaCO_{3(s)} + H_2O_{(aq)} + \text{am-}SiO_{2(s)} \tag{5}$$

Microbially induced mineralization is a potential mechanism to control fluid migration or seal wellbores via the bioprecipitation of calcium carbonate (Dejong et al., 2013; Phillips et al., 2013). The use of *Sporosarcina pasteurii* to improve oil recovery by modifying preferred flow paths in oil-bearing formations was proposed by Ferris and Stehmeier (1992) and most recently Phillips et al.

(2013) reviewed the utilization of biomineralization to increase wellbore cement integrity. *Sporosarcina pasteurii* produces urease as a metabolic byproduct and in the presence of urea and Ca^{2+}, deposition of calcium carbonate occurs (Fujita et al., 2000; Fujita et al., 2008; Mitchell and Ferris, 2006; Mitchell et al., 2008, 2010; Colwell et al., 2005; Phillips et al., 2013, 2015). Exploitation of this reaction in engineered systems is useful to strengthen unconsolidated porous media (Van Paassen, 2011) and reduce permeability of sandstone fractures (Phillips et al., 2015). Mitchell et al. (2013) found *S. pasteurii* to be metabolically active and capable of precipitating calcium carbonate in saline and porous synthetic media in the presence of supercritical CO_2 at 7.5 MPa and 32 °C. This work showed that bacterial ureolysis (hydrolysis of urea) led to increased pH (up to 9.1) and nucleation of calcite. The total amount of calcite precipitated was limited by mass transport of Ca^{2+} ions and urea.

Microbially produced urease catalyzes the hydrolysis of urea into carbonic acid and ammonia; carbonic acid and ammonia dissociate in water to form ammonia, hydroxide, and bicarbonate ions. Provided there is a calcium source, this reaction will lead to the subsequent precipitation of calcium carbonate as described in Eq. (6) (Mitchell et al., 2013). For *S. pasteurii* to be used at the field scale to effectively seal wellbores, its growth and ability to produce urease needs to be evaluated at conditions that will be found in wellbore environments, specifically high temperature, salinity, and pressure.

$$CO(NH_2)_2 + 2H_2O + Ca^{2+} \leftrightarrow 2NH_4^+ + CaCO_3 \qquad (6)$$
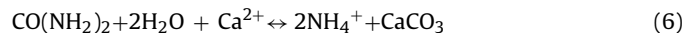
Class H Portland cement is commonly used in wellbores making it amenable to the reaction above in the presence of calcium enriched brine. Well temperatures can exceed 40 °C and pressure increases with depth. Phillips et al. (2015) demonstrated in laboratory experiments that pressures (4.5 MPa) in wells would not be detrimental to *S. pasteurii*'s ability to seal cracks in the cement. Further, moderate temperature (32 °C) and pressure (7.5 MPa) did not preclude this species from mediating the precipitation of $CaCO_3$ (Mitchell et al., 2013). However, much is left to be learned about the synergistic impacts of temperature, brine, and pressure on the growth and ability of *S. pasteurii* to precipitate $CaCO_3$ under the conditions where fractured sealing would be most beneficial to supercritical CO_2 storage. In both of the previously cited papers, the medium used to test the efficacy of *S. pasteurii* was a nutrient rich solution that is unlike the brine found in those aquifers most likely to be used for supercritical CO_2 injection. We investigate the mineralogical changes induced by *S. pasteurii* in cement bonded to Mt. Simon sandstone immersed in high salinity brine at various temperature and pressure conditions, and in the presence of supercritical CO_2. Supporting experiments were conducted on bacteria growing in a nutrient rich broth and brine, as well as precipitation on membrane filters and cement-sandstone samples to test the limiting factors on the growth of *S. pasteurii* in subsurface conditions.

2. Experimental methods

2.1. Sample preparation

To simulate *in situ* (down hole pressure and temperature) conditions in the experiments, we used a sandstone sample cored from the Mt. Simon formation, prepared raw Class H Portland cement, and prepared a brine solution to match that of the fluids in a target CO_2 injection site in the Mt. Simon formation. The brine was comprised of NaCl, $CaCl_2$, $MgCl_2$, and trace salt species (Table 1; based on Hazen core data, Illinois State Geological Survey). All sample conditions are described in Table 2. The Mt. Simon sandstone is a coarse grained sandstone that overlies Precambrian granite and underlies fine-grained Eau Claire Formation (c.f., Bonneville

Table 1
Top 5 salt species used to represent the Mt. Simon sandstone from the Illinois Basin at the expected 1220–1250 m depth (Hazen well data, Illinois State Geological Survey, 2010).

Simulated Mt. Simon Sandstone Illinois Basin Brine	Quantity, g/L
NaHCO$_3$	**0.84**
NaCl	**59.36**
MgCl$_2$	**5.71**
Na$_2$SO$_4$	**2.84**
CaCl$_2$	**18.85**
Total	**87.60**

et al., 2013). A core sample from the Mt. Simon Formation acquired 1198 m below land surface (provided by J. Szecsody, Pacific Northwest National Laboratory) was sub-cored into 1.3 cm diameter cylinders.

The raw Class H Portland cement powder (Lafarge) contained 64.5 wt.% tricalcium silicate (Ca_3SiO_5), 11.77 wt.% dicalcium silicate (Ca_2SiO_4), 13.24 wt.% calcium aluminoferrite (Ca_4AlFeO_5), 2.94 wt.% MgO, 2.8 wt.% SO_4^{2-}, and 0.16 wt.% total alkali content (Na_2O). This cement has no tricalcium aluminate ($Ca_3Al_2O_6$). The cement powder contained 0.62% free lime (CaO). The [water] loss on ignition (LOI) was computed to be 0.73, a value that is within acceptable ASTM limits. The cement slurry was prepared using a water-rock (w/c) ratio of 0.38 composed of 500 g dry cement powder and 190 mL of distilled water according to American Petroleum Institute (API) Recommended Practice RP10-B. The sandstone sub-cores were encased in a cement slurry, cured for 24 h in a humidity controlled room, removed from the mold, and subsequently immersed in a 30 °C Mt. Simon brine bath to cure for 28 days at 1) ambient pressure or 2) at 10 MPa (hydraulic or P_{CO_2} = 10 MPa) to simulate the expected pressure at the target injection site. All cores were cured at the pressure that they would be subjected to during the respective experiments. After the curing period, the cement-sandstone cores were cut into 1.3 cm slices for detailed imaging and characterization at ambient and high pressures and at variable temperatures, as described below.

2.2. Culture growth experiments at ambient conditions

Sporosarcina pasteurii (strain 11859) used for all experiments was obtained from the American Type Culture Collection (ATCC). We tested growth in 1) both a nutrient-rich broth, 2) in calcium-enriched Mt. Simon brine, and 3) on cement-sandstone cores immersed in Mt. Simon brine. An additional experiment quantified growth on membrane filters placed on top of an agar made with the nutrient-rich broth. The ideal growth medium for this strain (referenced as 'ATCC medium') is composed of 20.0 g yeast extract and 10.0 g ammonium sulfate in 1.0 L 0.13 M Tris Buffer (pH 9.0). The Tris Buffer was autoclaved (sterilized) prior to adding the yeast extract and ammonium sulfate, and then filter-sterilized using 0.2 μm syringe filters. All glassware used throughout the experiment was heat sterilized by autoclave. Early in the experiments, we observed rapid and abiotic precipitation of $MgHPO_4$ when an inoculum in ATCC medium was added to the brine as a result of brine-medium interactions (see sections 3.1 and 4.1). To prevent formation of $MgHPO_4$ crystals in subsequent experiments, an aliquot (0.5 mL to 1.0 mL) of the inoculum was centrifuged (1200 rpm for 10 min) to pellet the bacteria and then the supernatant medium was replaced with brine. The cell pellets were rinsed at least 3× with brine to remove all traces of the ATCC medium prior to inoculating the brine solution. Sterilized Mt. Simon brine was augmented with 1 or 10 g per liter of urea, as this substrate is needed for the hydrolysis reaction to occur over a 7 day period.

Table 2
Experimental conditions for culture growth experiments and rocking autoclave experiments.

Culture Growth Experiments						
Media	Solution	Solution	Filter + Solution			
Solution	Brine[b] + Urea	Brine[b] + Urea	Brine[b] + Urea			
Temperature (°C)	30	40	30			
Pressure (MPa)	ATS[c]	ATS[c]	ATS[c]			
Rocking	–	–	–			
Inoculum	*S. pasteurii*	*S. pasteurii*	*S. pasteurii*			
Rocking Autoclave Experiments						
Media	Cement + SS[a] + Solution	Cement + SS[a] + Solution	Cement + SS[a] + Solution	Cement + SS[a] + Solution	Cement + SS[a] + Solution	Cement + SS[a] + Solution
Solution	Brine[b] + Urea	Brine[b] + Urea	Brine[b] + Urea	Brine[b] + Urea	Brine[b] + Urea	Brine[b] + Urea
Temperature (°C)	30	30	30	40	30	40
Pressure (MPa)	10	10	10	10	10 [d]	10 [d]
Rocking	180°	180°	45°	45°	45°	45°
Inoculum	–	*S. pasteurii*	*S. pasteurii*	*S. pasteurii*	*S. pasteurii*	*S. pasteurii*

[a] Sandstone.
[b] Brine = Mt. Simon Sandstone (Illinois Basin).
[c] Atmospheric.
[d] Hydraulic pressure.

Bacterial cells in sub-samples from each treatment (e.g., ambient and high pressure conditions) were visualized by epifluoroescent microscopy and enumerated by direct cell counting. Aliquots from each treatment were preserved using formaldehyde (2% final concentration) and stored at 4 °C until counting. Briefly, each preserved sample was filtered through a black 25 mm diameter 0.2 μm cyclopore (Whatman) membrane filter. A glass-fiber backing filter (GF/F) was used beneath the membrane filter to produce an even distribution of the bacteria on the membrane. The bacteria on the filter were stained using Sybr Gold nucleic acid dye, visualized using an epifluoroescent microscope, and enumerated by direct counting. At least 10 frames and a total of 200 bacterial cells were counted per slide at 600× magnification. The software ImagePro was used to enumerate the bacteria on each slide. Automated enumeration was double-checked by direct visualization and counting. While growth curves are presented for ambient pressure, sequential sampling was not possible during high pressure rocking autoclave experiments (see below in section 2.3).

Sporosarcina pasteurii was also grown on cyclopore membrane filters to investigate morphological growth progression. For these experiments, ATCC media was inoculated with *S. pasteurii* and grown for 48 h at 30 °C to ensure that the bacterium was in the same growth phase for each replicate. A 1 mL aliquot of cell suspension was washed (as above) in brine to remove phosphate in the media. Then 2.5 μL of brine suspended bacteria were carefully drop-casted on a membrane (0.22 μm pore diameter) and placed on an agar petri dish with the ATCC growth medium in the agar. The petridishes were incubated at 30 °C for 72 h. A 5 mL brine solution containing 1 g/L urea was added to the petri dish for 60 s to precipitate calcium carbonate and stabilize the biofilm before being replaced by brine with variable urea concentrations. After incubation for 0.25, 4, 24 and 96 h the membranes were imaged by scanning electron microscopy (SEM) and scanning electrochemical microscopy (SECM). For a complete description of the SECM application, see Harris et al. (2016).

Bacterial biofilm formation and biomineralization on cement and sandstone was investigated using cylinders of sandstone encased in cement that were inoculated with *S. pasteurii*. Cement-sandstone samples prepared at 30 °C in Mt. Simon brine solution were placed in 99% ethanol for 15 min to sterilize the outer surfaces. We did not autoclave these samples to sterilize them as that would alter the chemical and physical structure of the cement. Cement-sandstone samples were dried in autoclaved beakers prior to being immersed in fresh brine containing either 1 or 10 g/L urea. The immersed samples were incubated at 30 °C for 7 days. At the end of the incubation period the samples were imaged (Canon T3i mounted to a Leica M80 stereoscope) and placed in a 2% formaldehyde solution to preserve the microbial community.

2.3. Rocking autoclave experiments

Cement-sandstone samples were cured at 30 °C or 40 °C and 10 MPa for 28 days, sterilized with ethanol, and dried in a N_2 purged desiccator for 8 h. As described above (Section 2.2) an inoculum culture of *S. pasteurii* in the ATCC medium was subjected to repeated centrifugation and brought back into suspension in sterile brine (1 mL, centrifuge, 15 mL of brine with 10 g/L urea respectively). An aliquot of the culture was removed and preserved with formaldehyde to obtain a time zero population count. A dual furnace ®CoreTest System rocking autoclave was used to conduct high pressure (hydraulic or P_{CO2} = 10 MPa) and temperature (30 and 40 °C) tests of inoculated and non-inoculated samples. The rocking system (45/180° rotation) was used to promote rock-water interactions.

Control experiments were run without inoculation of *S. pasteurii* for abiotic comparisons. For the biotic incubations, 14 mL of *S. pasteurii* culture was added to a Ti-flexible cell that contained the cement-sandstone sample. The remaining volume of the Ti-cell was filled with Mt. Simon brine solution for a 1:3:1 rock-water-gas ratio. The system was pressurized hydraulically, checked for leaks, and then heated to the desired temperature. After 16 h of operation, a 20 mL sample of fluid was taken from each Ti-cell, 20 mL (volume). CO_2 gas was fed into the system through a supercritical CO_2 booster pump to attain pressure of 10 MPa, and set to rock once the pressure was stable. After two weeks, autoclaves were stopped, a solution sample was taken under high pressure and temperature conditions using a Hamilton style glass syringe and the pH was measured immediately. This style of syringe as it allowed us to extract samples under pressure to minimize degassing prior to pH measurement. The autoclaves were then depressurized over a 2 h period. At this point an aliquot was collected and preserved with formaldehyde for determination of bacterial abundance. Cement-sandstone samples were removed from the Ti-cells and placed in a −20 °C freezer to prevent cement hydration and microbial activity prior to further analysis. No other aqueous chemistry was conducted due to the high total dissolved solid content of the brine and the dissolved ammonium analysis was inconclusive (Table 1).

2.4. Sample characterization

Sample analysis and characterization of phase changes in the Class H cement and Mt. Simon sandstone before and after incu-

bation experiments were completed using a petrographic optical microscope, a field emission (FE) FEI Inspect F scanning electron microscope (SEM), and a JEOL 7000F FE-SEM. Uncoated samples were examined with an accelerating voltage of 5–12 keV and a spot size 4.5 (dimensionless) to obtain high-resolution secondary electrons (SE) images. By combining backscatter electron (BSE) imaging and energy dispersive spectroscopy (EDS) we were able to acquire semi-quantitative elemental concentrations using the INCA software (Oxford). Specific samples were analyzed further with a wavelength-dispersive spectrometer (WDS) with standard errors and correction matrices for cement.

Growth of *S. pasteurii* on thin films was imaged by applying a ~50 μl drop of fixative (2.5% glutaraldehyde, 1% paraformalde-hyde in 0.1 M sodium cacodylate buffer) to the frozen filter. After 4 h at room temperature, the film was rinsed for 10 min in sodium cacodylate buffer. Samples were prepared for SEM by a serial dehydration of acetone (concentrations: 10%, 30%, 50%, 70%, 90%, and 100%) for 15 min and subsequently critical point dried. Dried filters were sputter coated with gold/palladium (60/40) for SEM. Images and electron dispersive spectrometry were acquired using a FEI Quanta 600F environmental SEM with an EDAX X-ray EDS detector at 8 kV with a spot size of 5.

Cementitious and mineral phases were characterized using X-ray diffraction (XRD). Diffraction patterns were collected using a Rigaku Ultima III with a 40 KV/40 mA Cu Kα source and a step speed of 1°θ/minute over a scan angle 2θ of 5° to 90°. The qualitative analysis of XRD data was performed using Jade v9.1.4 Plus software and the International Center for Diffraction Data (ICDD) pattern databases (ICDD, 2008).

3. Results

3.1. Culture growth at ambient pressure and 30/40 °C

In the first experimental trial, it was difficult to accurately calculate the growth rate of *S. pasteurii* because of the rapid precipitation of magnesium hydrogen-phosphate (200–500 μm in diameter) within minutes. This was the result of phosphate present in the media (Fig. 1). The media was re-evaluated, and reproducible growth rates in an ideal growth medium were determined (see Section 4.1 for more details on applications).

The synergistic impact of both temperature and brine solution were tested by ability of *S. pasteurii* growth at multiple temperatures in nutrient broth alone or in a brine solution. *Sporosarcina pasteurii* grew best in the nutrient broth (ATCC medium) at 30 °C and were stable at 40 °C, whereas the cell numbers attained in the Mt. Simon brine (with 1 g/L or 10 g/L urea added) were lower and more temperature dependent (Fig. 2). The density of the bacteria increased from 7.7×10^4 ($\pm 2.8 \times 10^4$ Standard Error; SE = Standard Deviation/$\sqrt{n}$) cells per mL to 1.1×10^6 ($\pm 6.5 \times 10^4$ SE) cells per mL within 24 h of inoculation in the nutrient broth at 30 °C. This growth rate slowed after 7 days with a low among replicate variance 3.79×10^6 per mL ($\pm 9.4 \times 10^4$ SE). At 40 °C the bacteria had a slower initial growth with higher variance among replicates; starting with the same inoculation density of 7.7×10^4 ($\pm 2.8 \times 10^4$ SE) cells per mL the population reached a density of 1.7×10^5 ($\pm 2.4 \times 10^4$ SE) cells per mL after 24 h. At this warmer temperature, the maximum density after 7 days was 1.4×10^6 ($\pm 1.0 \times 10^5$ SE) cells per mL, or ~38% of the final density at 30 °C.

In all scenarios containing the Mt. Simon brine, the number of cells declined from its initial inoculation concentration within the first 6 h before stabilizing at a lower concentration (Fig. 2). At 30 °C, this stabilization ranged between 3.0×10^4 and 4.0×10^4 cells per mL with a much higher among replicate variance for both the 1 and 10 g/L urea treatments. For example, at 7 days, the standard error

was 45% of the mean population density for 1 g/L urea and 30 °C treatment; this is also indicated by the much large error bars (Fig. 2). At 40 °C, there was again a rapid decrease after the inoculation with counts ranging $2.6–3.7 \times 10^4$ cells per mL in both brine and urea treatments. In the 40 °C treatment, the population did not recover from the initial reduction in concentration post-inoculation; the 1 g urea/L treatment was reduced to 1.0×10^4 ($\pm 0.9 \times 10^3$ SE) cells per mL after 7 days and in the 10 g urea/L no cells were visible even with repeated and extensive attempts to quantify them across all replicates at this time point. Our conservative minimum estimated detection limit was 130 cells per mL.

Total cell count numbers decreased from the initial inoculation concentration in brine (including urea) over 7 days, SEM images and analyses of cyclopore membrane filters inoculated with *S. pasteurii* immersed in the brine solution with low (1 g/L) and high (10 g/L) at 30 °C illustrates the rapid precipitation and progression of bioprecipitated matrix over 96 h (Fig. 3). SECM analyses demonstrated that calcium carbonate layer formed quickly after inoculation (<0.25 h) and the carbonate morphology becomes more pronounced after 96 h with a nodular appearance (Fig. 3 enlarged area with distinct crystals). Direct SECM measurements on the same samples, show a rapid increase in pH, from 6.9 up to 9.2 within the first 10 min of incubation, approximately ~200 μm above the biofilm. The average thickness of the measured biofilm was 95 ± 10 μm with topography ranging 20–87 μm as measured with a SECM (concurrent with this study, Harris et al., 2016).

3.2. Characterization of cement-sandstone substrates

The Mt. Simon sandstone is a mature, coarsely graded arenite, containing ~99% quartz (SiO_2-rich) bands with banded oxidized iron hydroxide and Fe-Ti-oxides (Fig. 4). Based on light microscopy and SEM, the typical grain size is ~401 ± 26 μm with 10% porosity. The pore space is filled with micaceous minerals, specifically muscovite ($KAl_2(AlSi_3O_{10})(OH)_2$). Other matrix minerals found in the sandstone as identified by SEM-EDS, SEM-WDS, and XRD include hematite (Fe_2O_3), ilmenite ($FeTiO_3$), $CuCO_3$, and trace (<1%) nichromite (($Ni,Co,Fe)(Cr,Fe,Al)_2O_4$) or ferrianchromite ($Fe^{2+}(Cr,Fe^{3+})_2O_4$) less than <5 μm across.

At the time of observation, the cement paste surrounding the sandstone contained approximately 25% unhydrated calcium silicates, calcium aluminate ferrites, and magnesium oxide phases that had not reacted with water to form $Ca(OH)_2$ or semi-gel like C–S–H (Fig. 4). The cement appears to have bonded fairly well (no apparent surface defects) to the sandstone; electron backscatter analysis revealed higher concentration of C–S–H at the interface. There were minor concentrations of dendritic hydrotalcite (($Mg_6Al_2(CO_3)(OH)_{16}\cdot4(H_2O)$)) on MgO grains.

3.3. Growth on cement-sandstone samples

In both brine treatments (1 and 10 g/L urea) at 30 °C at atmospheric pressure, a biofilm formed on the cement-sandstone samples that was white in appearance due to the deposition of calcium carbonate (Fig. 5). $CaCO_3$ deposition seemed to occur more rapidly at higher concentrations of urea as observed by the formation of the biofilm crust on the cement that extended into the sandstone surface (Fig. 5). At 1 g/L urea the colonies were smaller and more dispersed with ~17% surface area coverage, whereas at 10 g/L urea, the total area coverage was ~61% with larger, denser colonies determine by the ratio of detected pixels to total pixels in ImagePro. The biofilm and crust were measured to be 20–75 μm thick with distinct crystal morphologies in SEM. Fig. 6a shows that the top surface in contact with the bulk fluid had $CaCO_3$ polymorphs (aragonite and calcite), trace dolomite ($MgCa(CO_3)_2$), trace gypsum ($CaSO_4 \cdot 2H_2O$), and halite (NaCl); all phases were confirmed

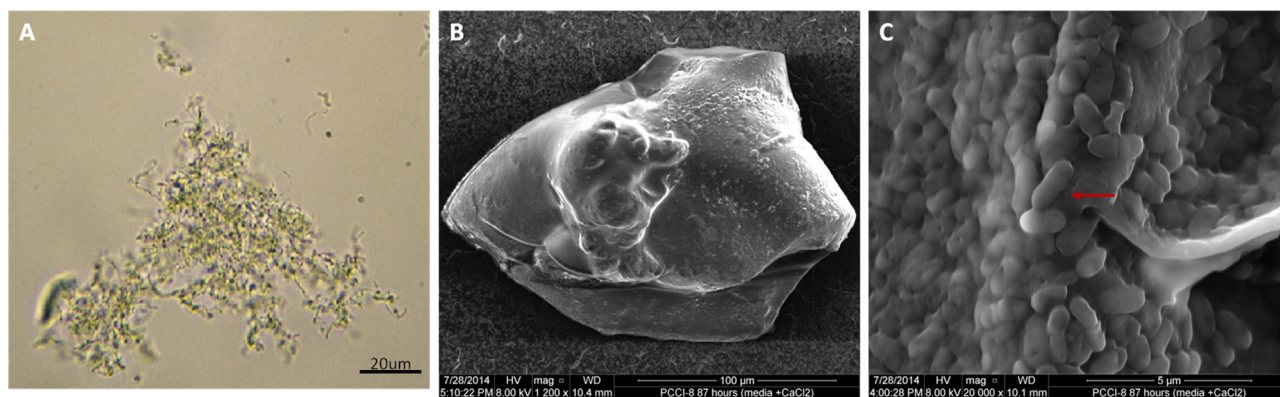**Fig. 1.** (A) Image of clumped *S. pasteurii* at 400×, after 24 h incubation in a media containing phosphate. (B) SEM-backscatter electron image showing the MgHPO₄ crystals (200–500 μm in diameter). The surface of these crystals are covered by a biofilm layer. (C) Rod-shaped microbes (red arrow) (1.15–1.7 μm) surrounding the MgHPO₄ crystals (For interpretation of the references to colour in this figure legend, the reader is referred to the web version of this article).

by XRD. *S. pasteurii* cells, either encased or adjacent to $CaCO_3$ polymorphs, were observed on the underside of the crust. SEM-BSE images showed that the rod-shaped bacteria which range in length between 6 and 7 μm and 3.1–3.3 μm in diameter appeared to be covered in a biotic-induced calcified crust as seen in Fig. 6 under atmospheric pressure in 10 g/L urea.

3.4. Growth at high pressure

The *S. pasteurii* populations survived and grew at 30 °C and high pressure (P_{CO2} = 10 MPa) as indicated by their population increasing 7.8 fold over the experiment. Over this same time, bulk fluid pH changed to 12 from 6.7. Injection of the supercritical CO_2 along with the rocking motion at 45° had no observable negative impact on *S. pasteurii* populations (Fig. 7). Furthermore, the bacterial density in the presence of CO_2 was comparable to the population (final density/initial density) at ambient pressure in the nutrient broth (Fig. 7). SEM images show that the biofilm nucleated on the cement with calcium carbonate crust had an average thickness of ≤20 μm at both temperatures as measured via SEM analysis (Fig. 8). The

cells in these films were <5 μm in length and 2 μm in diameter and had not been entirely encased by $CaCO_3$. However, at 40 °C, the bacterial cell numbers were lower than observed at 30 °C under supercritical CO_2 conditions; the density only increased by 60% (1.8×10^3–3.0×10^3 cells per mL) at 40 °C over the same period of time that population at 30 °C (863–4.0×10^4 cells per mL; Fig. 7). In this experiment, the pH of the solution increased to 11 in the 40 °C treatment.

Other factors such as rocking and incubation under hydraulic pressure had different results on population growth and stability. For example, at 30 °C, under supercritical CO_2 conditions with 180° of rocking, the population growth rate was much slower ($1.8 \times$ increase in cell density over the duration of the experiment, or from 4.4×10^3 to 8.4×10^3 cells per mL) than the sample that experienced 45° rocking ($46 \times$ increase in cell density or 863–4.0×10^4 cells per mL). At 40 °C, the sample was broken up and formed a slurry due to the 180° rocking motion, making it difficult to accurately enumerate bacterial cells in the sample as the fragments occluded the view of the microscope. In addition, the high pressure hydraulic treatments (no CO_2) at 30 °C had a final cell density
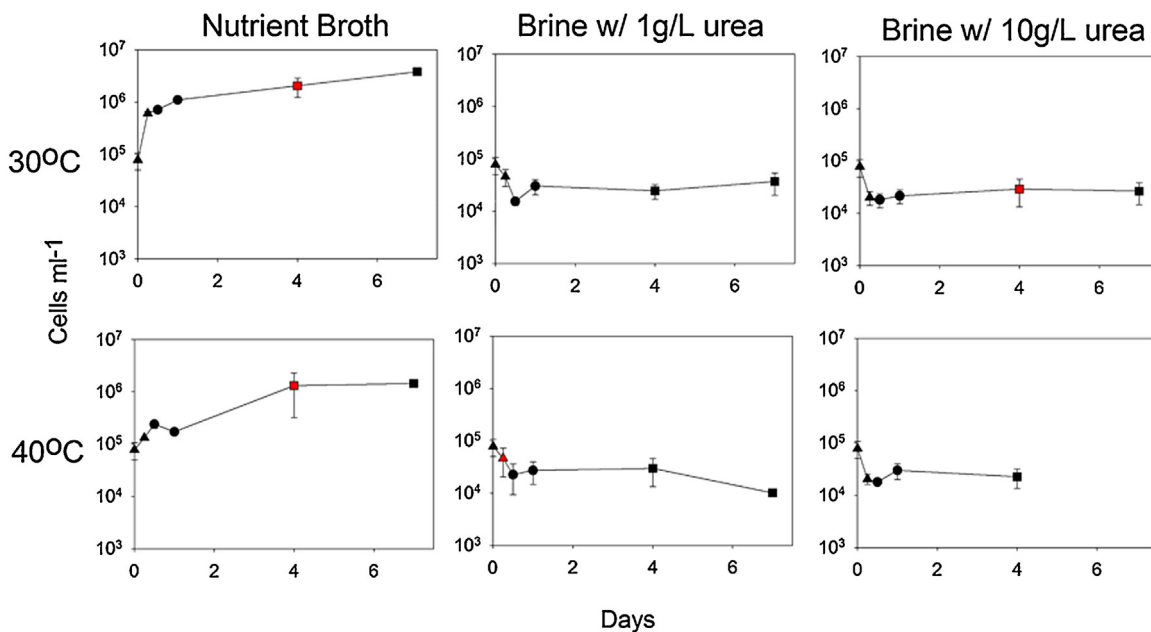

Fig. 2. *S. pasteurii* growth (log cell/mL up to 7 days) at different temperatures and growth media. Error bars are range of two replicates. *Sporosarcina pasteurii* cell counts in the nutrient broth increased up to 7 days with low variability. However, inoculation in the brine displayed lower cell counts with temperature dependence. Population was below detection (estimated to be 130 bacteria per mL) after 4 days at 40 °C at 10 g/L in all three replicates.
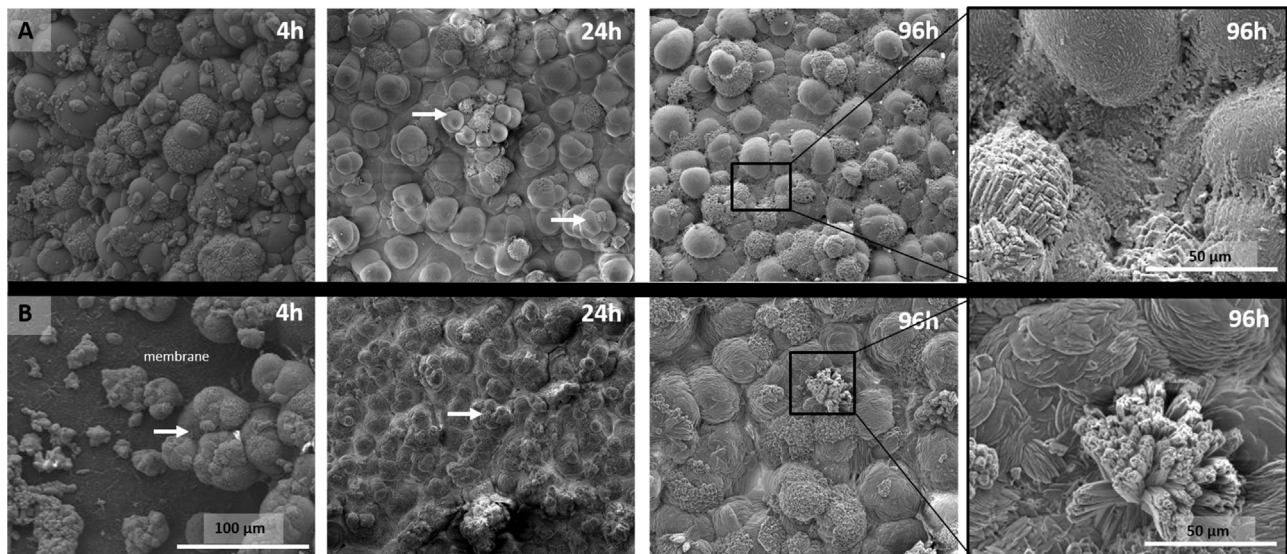
Fig. 3. SEM micrograph of biofilm growth on cellulose membrane filters in brine media with low and high urea at 30 °C at ambient pressure up to 96 h. The small round topographical features (arrows) represent calcium carbonate precipitation on the surface of the bacterial clusters. (A) High urea (10 g/L) (B) Low urea (1 g/L). Scale bar for all images is 100 μm except noted in the enlarged images as 50 μm.

that increased 7.8 fold (from 6.9×10^3 to 5.4×10^4 cells per mL) whereas the 45° rocking 30 °C with P_{CO2} conditions had the afore-mentioned 46 fold increase in cell density. However, this may have been an artifact of the especially low inoculation density in the 30 °C treatment with P_{CO2}. In the absence of CO_2 at 40 °C, the cell density increase was nearly double (from 7.9×10^3 to 3.3×10^4 cells per mL) of that observed in the P_{CO2} samples at 40 °C (from 1.8×10^3 to 3.0×10^4 cells per mL; Fig. 7). Of note, each of these treatments had final densities of $\sim 10^4$ cells per mL. The abiotic sample, which did not contain bacteria pre- or post-experiment, was omitted from the bacterial comparison as there were no bacteria observed.

3.5. Abiotic and biotic carbonation

Carbonates form naturally on cement in the presence of CO_2. However, there are key differences between the abiotic cement subjected to CO_2 (CO_2-saturated fluid and supercritical CO_2) and cement samples inoculated with *S. pasteurii* (Figs. 9 and 10). The abiotic carbonated cement was composed primarily of poly-crystalline vaterite (1–2 μm) and well distributed rhombohedral calcite (~ 2 μm) that replaced the cementitious phases $Ca(OH)_2$ and C–S–H. At both ambient and P_{CO2} = 10 MPa, samples inoculated with *S. pasteurii* displayed bio-induced acicular and orthorhombic aragonite (3–5 μm), rhombohedron calcite, and polycrystalline vaterite (<1 μm). Petrographic analysis and electron microscopy show that the biofilm and subsequent biomineralization initiated in cement and extends onto the sandstone surface.

4. Discussion

4.1. Biogenic precipitation: ambient pressure

The rapid precipitation of $MgHPO_4$ demonstrates the impor-tance of understanding complex brine chemistry, specifically brines containing phosphate. Furthermore, it highlights the need to understand the components of culture media for application in lab-oratory experiments and field applications. In this case, if a large inoculum of *S. pasteurii* was injected down wellbore in the ideal growth medium, upon reaching the *in situ* brine an abiotic precipi-tate would likely block the well rather than distribute the bacteria
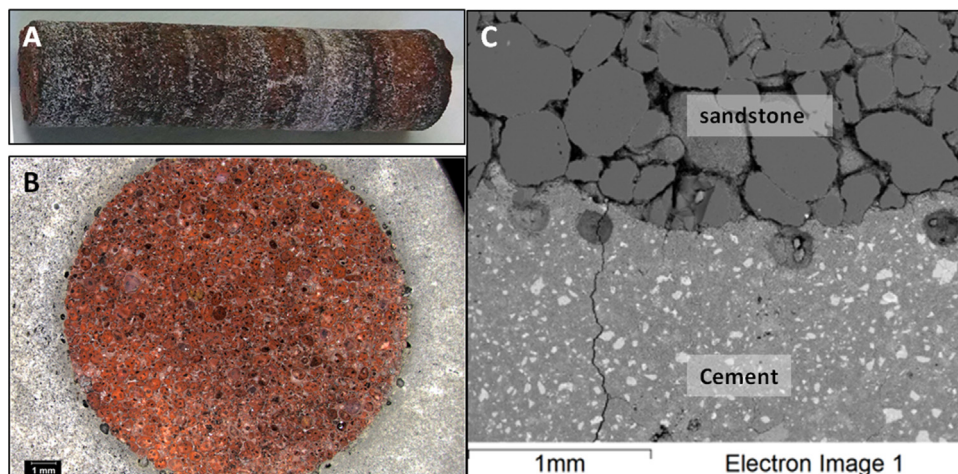

Fig. 4. (A) 4" Mt. Simon sandstone sub-core. (B) Reflected photomicrograph of oxidized rust red Mt. Simon sandstone encased in grey Lafarge Class H cement. (C) SEM-BSE image of the cement-sandstone interface. (For interpretation of the references to colour in this figure legend, the reader is referred to the web version of this article.)
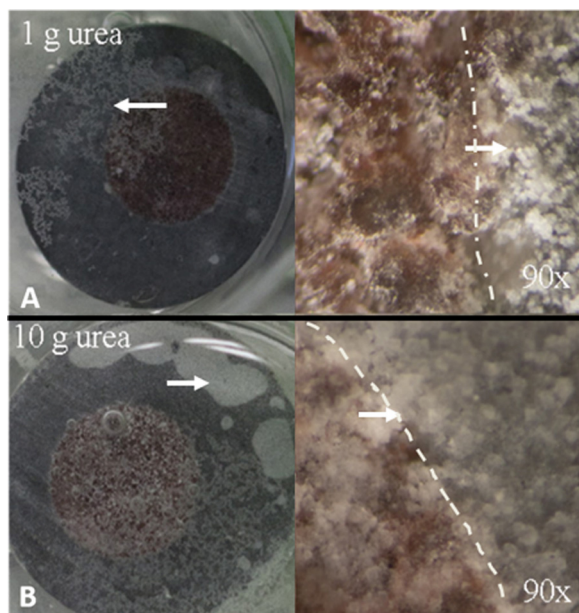
Fig. 5. Growth of *S. pasteurii* on the cement-sandstone samples (interface dashed line) immersed in (A) 1 g/L or (B) 10 g/L urea concentrations and subsequent microbe colony growth (white arrow). Magnification increases from left to right with the maximum magnification ~90× on a Canon T3i mounted to a Leica M80 stereoscope. There is ~17% biofilm surface area at 1 g/L and ~61% biofilm surface area at 10 g/L with the majority of the biofilm attached to the cement as calculated using ImagePro.

taken advantage of the cement for initial nucleation sites using calcium from $Ca(OH)_2$ and C–S–H and inducing a higher concentration (~17% versus ~61% surface area coverage at 1 and 10 g/L urea respectively) of $CaCO_3$ as seen in Fig. 5. Another example of microbially-induced mineral precipitation is the presence of a Mg-carbonate, chemical similar to dolomite as identified by SEM-EDS found protruding from the cement pore space only in samples inoculated with *S. pasteurii* under ambient pressure (Fig. 6). SEM images support that microbes could be associated with the dolomite precipitation and could be indicative that the microorganisms used magnesium-enriched brine. The mechanism of the dolomite precipitation warrants further examination. Furthermore, a crustal layer of halite (NaCl) was also present; however, we could not confirm if NaCl was produced as a result of metabolic activity, depressurization, or sample preparation.

Based on our results, the efficacy of using *S. pasteurii* to seal wellbores appears to be limited by temperature and is less sensitive to urea concentrations. At 40 °C in the Mt. Simon brine, there was strong evidence that the population had a lower stable population density, at low urea concentrations, or was not viable at the higher urea concentrations. It is unclear why the concentration of urea impacted the growth of the species. We conclude that the species can live at 40 °C for short durations, but the increased variance in population growth rates was indicative of a population under stress.

Cells encased in $CaCO_3$ are one potential mechanism that would lead to the observed discrepancy in population density in high urea samples and unable accurately count them. Microbially-induced carbonate precipitation leading to bacterial encapsulation has been suggested by Cuthbert et al. (2012) and verified by SECM. If encapsulation was the reason we saw reduced growth in the high urea and brine treatments, then we would expect to see some cells present throughout the experimentation. This was not seen in the 40 °C, brine and high urea treatment and instead, even with an exhaustive search across all replicates, we detected no cells.

Bacteria encapsulated in a non-transparent shell (e.g. carbonate) are difficult to enumerate using standard light microscopy methods. While optical density may have been an alternative approach to the nucleic acid stain we employed, both of these approaches can be heavily influenced by mineral precipitation and cellular density. While the nucleic acid stain used does not only stain viable cells, it will not stain lysed cells making it useful as a proxy for cells that are intact. Future approaches could quantify cellular concentration using lipid or gene abundance techniques, however these approaches also have a difficult time separating intact vs. non-
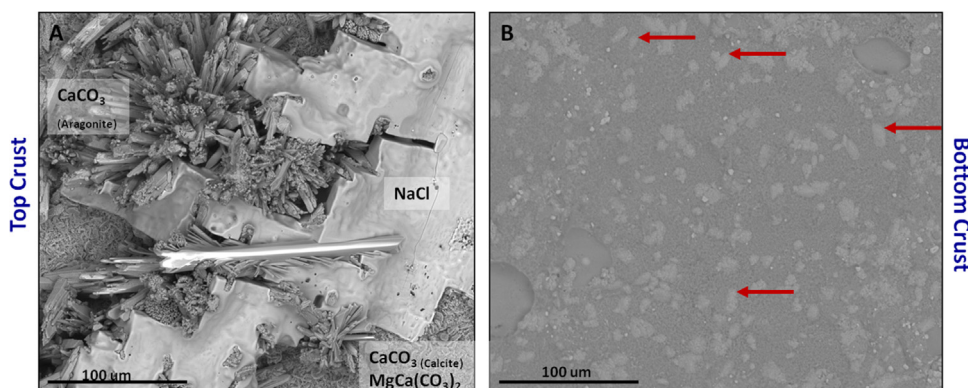
throughout the area targeted for repair by the bacteria. Once phosphate was eliminated, the high concentration of calcium in the Mt. Simon brine and from the cement resulted in calcium carbonate biomineralization in a more desired, controlled reaction. We did not compare the growth of *S. pasteurii* in our "ideal" growth medium to that used in other studies (e.g. Phillips et al., 2013); it is important to recognize that abiotic precipitation of $MgHPO_4$ should be considered when choosing the correct medium to use when introducing *S. pasteurii* to a well. Based on the findings of Tobler et al. (2012) it is possible to avoid the use of media and subsequent phosphate precipitation by injecting cell lysate.

SEM-EDS, SEM-WDS, and XRD identification of the carbonate species demonstrated that *S. pasteurii* enabled biotic mineralization at 30 °C in brine containing urea (see Appendix A). Specifically rhombohedral calcite, orthorhombic (hexagonal) and acicular aragonite, gypsum, and dolomite precipitated on the cement-sandstone surface (Figs. 6 and 10). *Sporosarcina pasteurii* appears to have

Fig. 6. Effect of culture growth on cement-sandstone surfaces at atmospheric pressure in a brine augmented with 10 g/L urea. (A) Several types of $CaCO_3$, (acicular aragonite and calcite) and $MgCa(CO_3)_2$ (dolomite). These minerals are not seen under abiotic conditions. (B) Underside of the biogenic crust with calcified features consistent with microbial cells (6–7 μm in length and 3.1–3.3 wide) (red arrows). (For interpretation of the references to colour in this figure legend, the reader is referred to the web version of this article.)
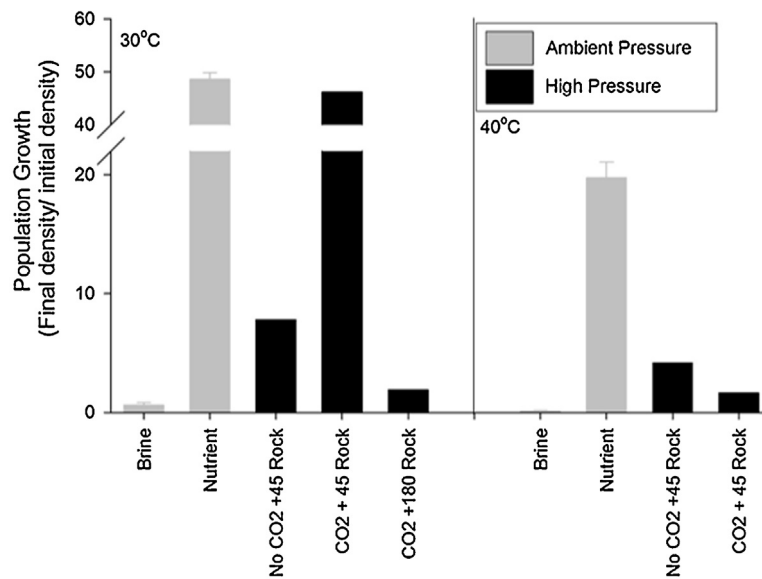
Fig. 7. The change in population growth as indicated by the final/initial density of *S. pasteurii* over incubations at both ambient (grey) and high pressure experiments (black) of the lab experiments from Section 3. The addition of CO_2 gas and degree of rocking (45 or 180°) is annotated.

intact cells. Our enumeration approach has limitations, but are consistent across all experimental treatments.

SEM images taken at various intervals (0.25, 4, 24, and 96 h) on a membrane filter inoculated with *S. pasteurii* in brine media illustrated precipitation of carbonate with time (Fig. 3). In addition, SECM measurements that as the local pH increased from 6.9 to 9.2 (within 10 min), indicating an extremely rapid ureolysis leading to deposition of calcite. These results are consistent with previous publications documenting a pH increase and calcite precipitation in cultures of *S. pasteurii* (which was limited by mass transport of Ca^{2+} and urea) seen in Mitchell et al. (2013). Our results add to the previous findings in that we document a bio-encasing effect of the cultures, limiting further growth and biomineralization (e.g. Mitchell et al., 2013; Cuthbert et al., 2012). Such time-point observations are key to the design of field tests, and suggest that inoculation of test boreholes be done in short time steps rather than expecting long-term activity for a given large pulse of inoculants. Such an approach was taken by Phillips et al. (2013) who found a significant decrease in permeability in a sandstone core following the sequential addition of urea after inoculation by *S. pasteurii*.

Similar approaches need to be further tested at both high pressure (e.g. Phillips et al., 2013), high pressure and temperature (Mitchell et al., 2013), and in a brine solution (this study). As a result this species continues to hold promise for sealing wellbores in shallow (not too warm) CO_2 abatement sites, as well as the other diversity of bioengineering roles that urease hydrolyzing bacteria may perform (reviewed in Phillips et al., 2015).

4.2. Biogenic precipitation: high pressure and temperature

Neither the increased pressure expected at wellbore depths nor the injection of supercritical CO_2 negatively impacted biomineralization induced by *S. pasteurii*, further supporting that this species could act as a component of a mitigation strategy for leaky wellbores targeted for carbon sequestration. During 2 weeks in a rocking autoclave at 30 °C and P_{CO2} = 10 MPa, the microbial colonies formed an organic-rich biofilm as identified by SEM-EDS that led to the formation of a globular $CaCO_3$ crust (Figs. 8–10). As observed in the ambient pressure tests, colonization appeared to preferentially occur on the cement surface and extend across the interface to the
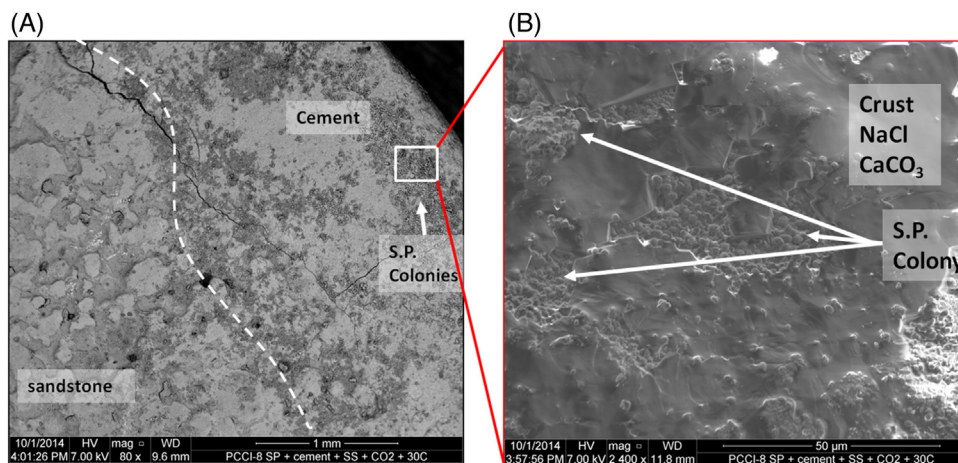

Fig. 8. (A) SEM images of cement-sandstone surfaces following 2 week incubation in a rocking autoclave at 30 °C and P_{CO2} = 10 MPa. Dark patches at the right are a biofilm with calcium carbonate, indicative of growth and cementation by *S. pasteurii*, which is more prevalent on the cement substrate. (B) Enlargement of colonies that encase themselves within a $CaCO_3$ crust.
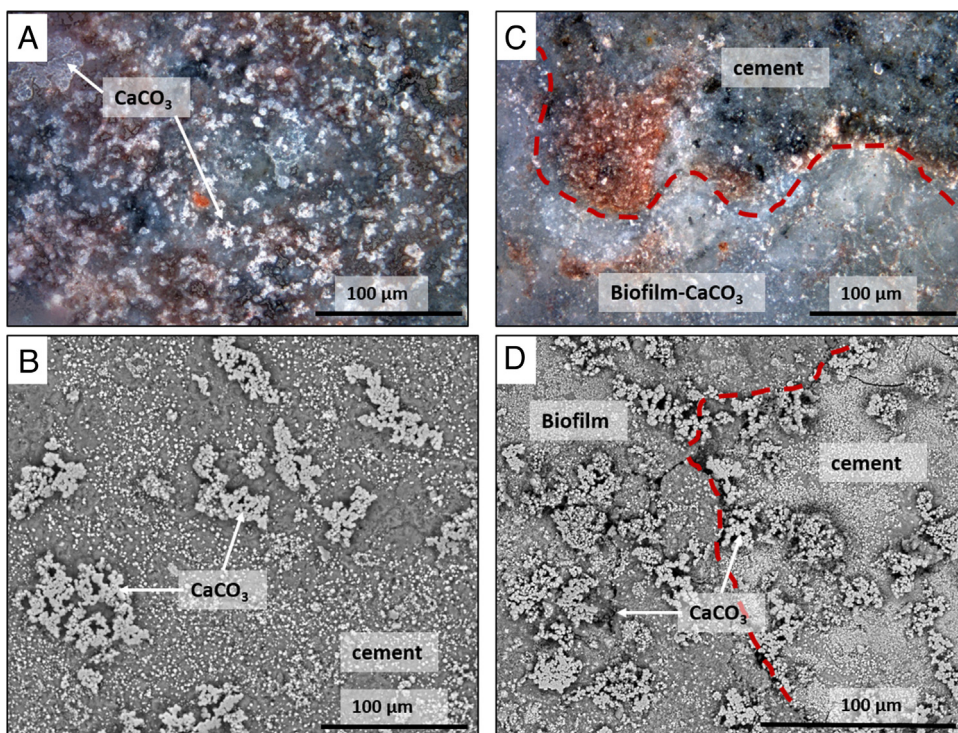
Fig. 9. Reflected microphotographs and SEM-BSE comparison between experiments conducted at 30 °C under P_{CO2} = 10 MPa without (A, B) and with (C, D) microbial inoculation (dashed line shows biofilm boundary). SEM-BSE images comparing (B) the presence of distributed $CaCO_3$ in the abiotic specimen and (D) distinct crystal structures when sample was incubated with *S. pasteurii*.

sandstone. The presence of *S. pasteurii* initiated the deposition of several phases of $CaCO_3$: aragonite, calcite, and vaterite. There are several notable differences of the biomineralization between ambient and high pressure. The first is the size of the twinning aragonite crystals; at higher pressure, the twinned aragonite crystals are significantly smaller (20 ± 8 μm as compared to 90 ± 33 μm clusters). Secondly, the microbial colonies are partially encased in secondary minerals. It was difficult to determine if the microbial colonies filled and "healed" fractures at P_{CO2}.

It is important to note that under pressure with supercritical CO_2, *S. pasteurii* was able to at least increase in density and lead to the precipitation of $CaCO_3$, which is indicative of it producing the urease enzymes. As the morphotype is distinct between biologically and non-biologically mediated precipitates, it is plausible that living populations led to this observed effect. This is comparative to ureolytic activity under anoxic conditions in which the precipitation is based on the presence of enzymes within the system (Tobler et al., 2011; Cuthbert et al., 2012). While other studies have found that the introduction of supercritical CO_2 under pressure can lead to a sterilization effect on certain taxa (e.g. Mitchell et al., 2008), we observed inhibition of growth at increased temperature and pressure and that *S. pasteurii* was able to survive under these conditions.

The population growth increased 46-fold over the duration of the experiment under P_{CO2} = 10 MPa [45° rocking] and are comparable to the cell counts observed after 7 days in the ideal growth medium at 30 °C (Fig. 7). Petrographically, there is less biogenic precipitation at 30 °C and P_{CO2}, but cell data demonstrates that *S. pasteurii* appeared to be stable during CO_2 injection. *Sporosarcina pasteurii* appears to be limited by temperature as the population growth of *S. pasteurii* was reduced 28 times at 40 °C compared to 30 °C at high P_{CO2} conditions. However, at 40 °C (P_{CO2}) the final population density was 1.6 times its initial concentration as such the population was still able to grow. As seen in previous studies (Mitchell et al., 2013), this study showed that the injection of *S.*

pasteurii into shallow wellbore depths and at lower temperatures (<40 °C) could help to improve compromised wellbore cements; it may be possible to seal fractures in a few days in wellbores where temperature is >40 °C. It is important to note that many of sites for potential supercritical CO_2 injection are at a minimum 40 °C, and thus this study is an important step forward in testing the efficacy of using *S. pasteurii* to seal wellbores in such regions. Modeling future high pressure and temperature off the work of Phillips et al. (2013), Ebigbo et al. (2010), and Mitchell et al. (2013), with a strategy of sequential injection may likely lead to the most effective approach to utilizing *S. pasteurii* for sealing wellbores.

4.3. Comparison between abiotic and biotic carbonation

S. pasteurii appeared to play an important role in bioprecipitation of aragonite and dolomite; *S. pasteurii* had an impact on the pH of the bulk solution where the biogenic pH was >11 compared to the abiotic pH of 9. Petrographic examination of the biotic surfaces found defined crystallization on the cement surface attributed to the presence of a biofilm. The biofilm enhanced the formation of calcium carbonate as also seen by Cunningham et al. (2009, 2011) and Mitchell et al. (2013); the extent of the bio-induced mineralization was not evident in abiotic samples (Figs. 9 and 10). It is feasible, that as the cement continued to hydrate, the cement pore solution increased in localized calcium to increase alkalinity and enhance carbonate deposition. The crystal structure of the calcium carbonate in the biotic treatments compared to that of the abiotic treatments varied considerably. The precipitation of vaterite, a metastable calcium carbonate, is more dominant than calcite in samples exposed to only supercritical CO_2, while the presence of the *S. pasteurii* resulted in a more stable crystalline form of aragonite and calcite. In agreement with our results, Abo-El-Enein et al. (2012) also found rhombohedral calcium carbonate depositions by *S. pasteurii* exposed to calcium chloride. However, the duration of CO_2 injection was limited to 2 weeks; other studies have indicated
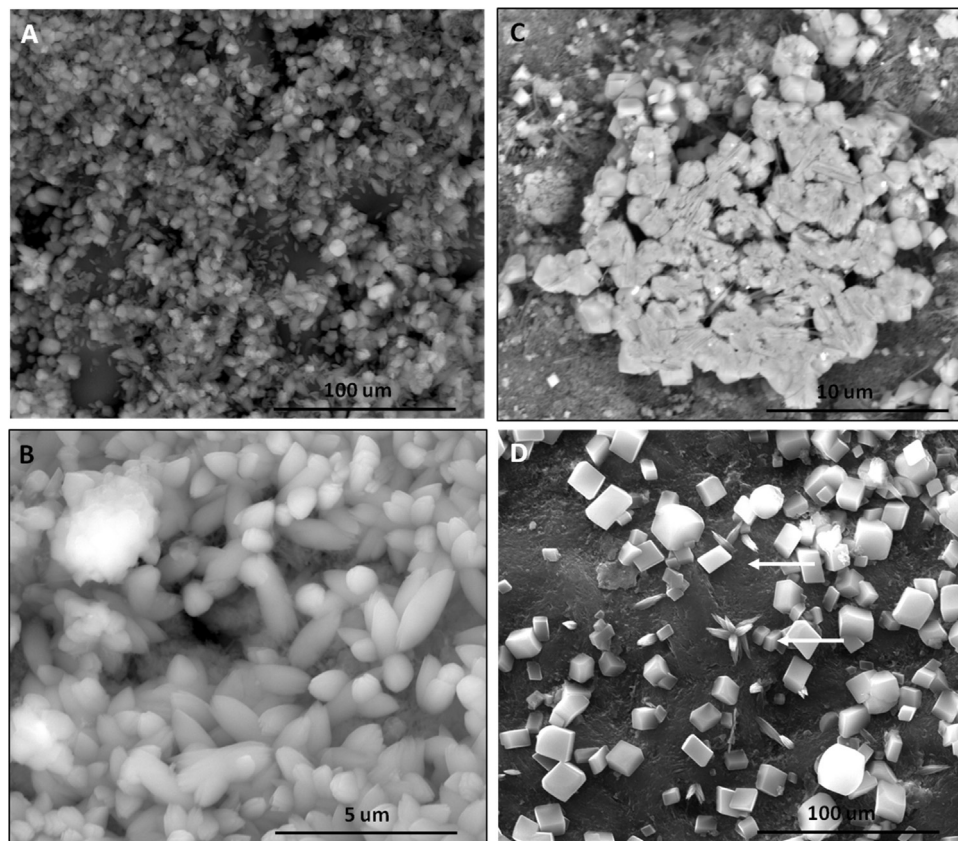
Fig. 10. Additional SEM images showing the difference between abiotic (A, B) and biotic (C, D) incubations in the rocking autoclave at 30 °C and 10 MPa P_{CO2}. (A) Overall view of secondary $CaCO_3$ precipitation. (B) Close up view of secondary $CaCO_3$ precipitation (A) Mineral replacement of $Ca(OH)_2$ forming polycrystalline vaterite and calcite. (C) Clustered hexagonal $CaCO_3$ (D) Rhombohedron calcite, orthorhombic aragonite, and acicular aragonite (arrows).

calcite as typically dominant in cement carbonation with lower concentrations of vaterite and longer test durations (e.g. Verba et al., 2014; Kutchko et al., 2008). Future research is required to understand if the chemical reaction is impacting the crystal lattice or if there is preferred orientation in the presence of *S. pasteurii*.

5. Conclusions

Our investigation of *S. pasteurii* growth in a synthetic brine that mimics the Illinois Basin and on Mt. Simon sandstone encased in Class H Portland cement, led to the following conclusions:

- Phosphate in media prompted rapid crystallization of $MgHPO_4$. This is an important consideration when designing a suitable *S. pasteurii* culture in laboratory bench experiments and scaling up to field applications.
- At atmospheric pressures, *S. pasteurii* were stable in high chloride brine solutions, but performed best at temperatures of 30 °C. The populations appeared to have reduced growth at $\geq$40 °C, but were stable for up to 4 days and thus could facilitate the rapid sealing of wellbore cement at temperatures found in certain wellbore regions.
- *S. pasteurii* is actively modifying the deposition of $CaCO_3$ on carbonate through its ureolytic activity at high pressure in brine environments. Biomineralization resulted in well crystallized $CaCO_3$ polymorphs, notably aragonite, and $MgCa(CO_3)_2$ as analyzed in SEM-EDS and XRD.
- At 30 °C under P_{CO2} = 10 MPa, *S. pasteurii* promoted additional $CaCO_3$ precipitation compared to abiotic samples. This environmental resilience is encouraging as *S. pasteurii* may be better adapted to the supercritical CO_2 conditions subject to respective temperatures.
- It is feasible that biogenic carbonation could improve wellbore integrity in carbon sequestration settings and could repair surface defects of the cement. Further research needs to be completed to understand if biomineralization can "heal" fractures and to document the optimal conditions for field implementation.

Disclaimer

Acknowledgments

Appendix A. Supplementary data

Supplementary data associated with this article can be found, in the online version, at http://dx.doi.org/10.1016/j.ijggc.2016.03.019.

References

Abo-El-Enein, S.A., Ali, A.H., Talkhan, Fatma N., Abdel-Gawwad, H.A., 2012. Utilization of microbial induced calcite precipitation for sand consolidation and mortar crack remediation. HBRC J. 8 (3), 185–192.

Barlet-Gouedard, V., Rimmele, G., Porcherie, O., Quisel, N., Desroches, J.A., 2009. Solution against well cement degradation under CO_2 geological storage environment. Int. J. Greenh. Gas Control 3, 206–216.

Bonneville, A., Gilmore, T., Sullivan, C., Vermeul, V., Kelley, M., White, S., Appriou, D., Bjornstad, B., Gerst, J., Gupta, N., Horner, J., McNeil, C., Moody, M., Rike, W., Spane, F., Thorne, P., Zeller, E., Zhang, F., Hoffmann, J., Humphreys, K., 2013. Evaluating the suitability for CO_2 storage at the FutureGen 2.0 Site, Morgan County, Illinois, USA. Energy Procedia 37, 6125–6132.

Colwell, F.S., Smith, R.W., Ferris, F.G., et al., 2005. Microbially-mediated subsurface calcite precipitation for removal of hazardous divalent cations: microbial activity, molecular biology, and modeling. In: Berkey, E., Zachary, T. (Eds.), Subsurface Contamination Remediation: Accomplishments of the Environmental Management Science Program, 904. American Chemical Society, Washington, pp. 117–137.

Cunningham, A.B., Gerlach, R., Spangler, L., Mitchell, A.C., 2009. Microbially enhanced geologic containment of sequestered supercritical CO_2. Energy Procedia 1, 3245–3252.

Cunningham, A.B., Gerlach, R., Spangler, L., Mitchell, A.C., Parks, S., Phillips, A., 2011. Reducing the risk of wellbore leakage of CO_2 using engineered biomineralization barriers. Energy Procedia 4, 5178–5185.

Cuthbert, M.O., Riley, M.S., Handley-Sidhu, S., Renshaw, J.C., Tobler, D.J., Phoenix, V.R., Mackay, R., 2012. Controls on the rate of ureolysis and the morphology of carbonate precipitated by *S. pasteurii* biofilms and limits due to bacterial encapsulation. Ecol. Eng. 41, 32–40.

Dejong, J.T., Burbank, M., Kavazanjian, E., et al., 2013. Biogeochemical processes and geotechnical applications: progress, opportunities and challenges. Geotechnique 63, 287–301.

Duguid, A., Radonjic, M., Scherer, G.W., 2011. Degradation of cement at the reservoir/cement interface from exposure to carbonated brine. Int. J. Greenh. Gas Control 5 (6), 1413–1428.

Ebigbo, A., Helmig, R., Cunningham, A.B., Class, H., Gerlach, R., 2010. Modeling biofilm growth in the presence of carbon dioxide and water in the subsurface. Adv. Water Resour. 33 (7), 762–781.

Ferris, F.G., Stehmeier, L.G., Bacteriogenic mineral plugging. US Patent Office. Pat. No. 5, 143, 155. TX. (1992).

Fujita, Y., Ferris, F.G., Lawson, R.D., Colwell, F.S., Smith, R.W., 2000. Calcium carbonate precipitation by ureolytic subsurface bacteria. Geomicrobiol. J. 17, 305–318.

Fujita, Y., Taylor, J.L., Gresham, T.L., et al., 2008. Stimulation of microbial urea hydrolysis in groundwater to enhance calcite precipitation. Environ. Sci. Tech. 42, 3025–3032.

Gasda, S., Celia, M., Wang, J., Duguid, A., 2013. Wellbore permeability estimates from vertical interference testing of existing wells. Energy Procedia 37, 5673–5680.

Harris, D., Ummadi, J., Thurber, A., Alleau, Y., Verba, C., Colwell, F., Torres, M., Koley, D., 2016. Real-time monitoring of calcification process by *Sporosarcina pasteurii* biofilm. Analyst, http://dx.doi.org/10.1039/C6AN00007J.

2010. Illinois Geological Survey. Hazen Data from Illinois Water Well (ILWATER). https://www.isgs.illinois.edu/ilwater.

Kutchko, B.G., Strazisar, B.R., Lowry, G.V., Dzombak, D.A., Thaulow, N., 2008. Rate of CO_2 attack on hydrated class H well cement under geologic sequestration conditions. Environ. Sci. Technol. 42 (16), 6237–6242.

McGrail, B.P., Schaef, H.T., Ho, A.M., Chien, Y.-J., Dooley, J.J., Davidson, C.L., 2006. Potential for carbon dioxide sequestration in flood basalts. J. Geophys. Res. 111.

Mitchell, A.C., Ferris, F.G., 2006. The influence of *Bacillus pasteurii* on the nucleation and growth of calcium carbonate. Geomicrobiol. J. 23, 213–226.

Mitchell, A.C., Phillips, A., Kaszuba, J., Hollis, H.K., Gerlach, R., Cunningham, A., 2008. Resilience of planktonic and biofilm cultures to supercritical CO_2. J. Supercrit. Fluids 47, 318–325.

Mitchell, A.C., Dideriksen, K., Spangler, L., Cunningham, A., Gerlach, R., 2010. Microbially enhanced carbon capture and storage by mineral-trapping and solubility-trapping. Environ. Sci. Technol. 44, 5270–5276.

Mitchell, A.C., Phillips, A., Schultz, L., Parks, S., Spangler, L., Cunningham, A.B., Microbial, R., 2013. Microbial $CaCO_3$ mineral formation and stability in an experimentally simulated high pressure saline aquifer with supercritical CO_2. Int. J. Greenh. Gas Control 15, 86–96.

Phillips, A.J., Gerlach, R., Lauchnor, E., Mitchell, A.C., Cunningham, A.B., Spangler, L., 2013. Engineered applications of ureolytic biomineralization: a review. Biofouling 29, 715–733.

Phillips, A.J., Eldring, J., Hiebert, R., Lauchnor, E., Mitchell, A.C., Cunningham, A., Spangler, L., Gerlach, R., 2015. Design of a meso-scale high pressure vessel for the laboratory examination of biogeochemical subsurface processes. J. Petrol. Sci. Eng. 125, 55–62.

Taylor, H.F.W., 1997. Cement Chemistry. Academic Press, New York.

Tobler, D.J., Cuthbert, M.O., Greswell, R.B., Riley, M.S., Renshaw, J.C., Handley-Sidhu, S., Phoenix, V.R., 2011. Comparison of rates of ureolysis between *Sporosarcina pasteurii* and an indigenous groundwater community under conditions required to precipitate large volumes of calcite. Geochim. Cosmochim. Acta 75, 3290–3301.

Van Paassen LA Bio-mediated ground, 2011. improvement: from laboratory experiment to pilot applications. ASCE Geotech. Spec. Publ. 211, 4099–4108.

Verba, C.A., O'Connor, W., Rush, G., Palandri, J., 2014. Basalt and sandstone host rock with class H Portland cement under CO_2 sequestration conditions. Int. J. Greenh. Gas Control 23, 119–134.